Geophysical Journal International

Supplementary Material for

From strain to displacement: using deformation to enhance distributed acoustic sensing applications

Alister Trabattoni[1], Francesco Biagioli[2], Claudio Strumia[3], Martijn van den Ende[1], Francesco Scotto di Uccio[3], Gaetano Festa[3], Diane Rivet[1], Anthony Sladen[1], Jean Paul Ampuero[1], Jean-Philippe Métaxian[2] and Éléonore Stutzmann[2]

[1] *Université Côte d'Azur, Observatoire de la Côte d'Azur, CNRS, IRD, Géoazur, France*
[2] *Institut de Physique du Globe de Paris, Université Paris Cité, Paris, France*
[3] *Università di Napoli Federico II, Complesso University Monte S. Angelo, Napoli, Italy*

Content of this file

Figures S1 to S4.

Introduction

This document provides additional simulations and technical filtering details.

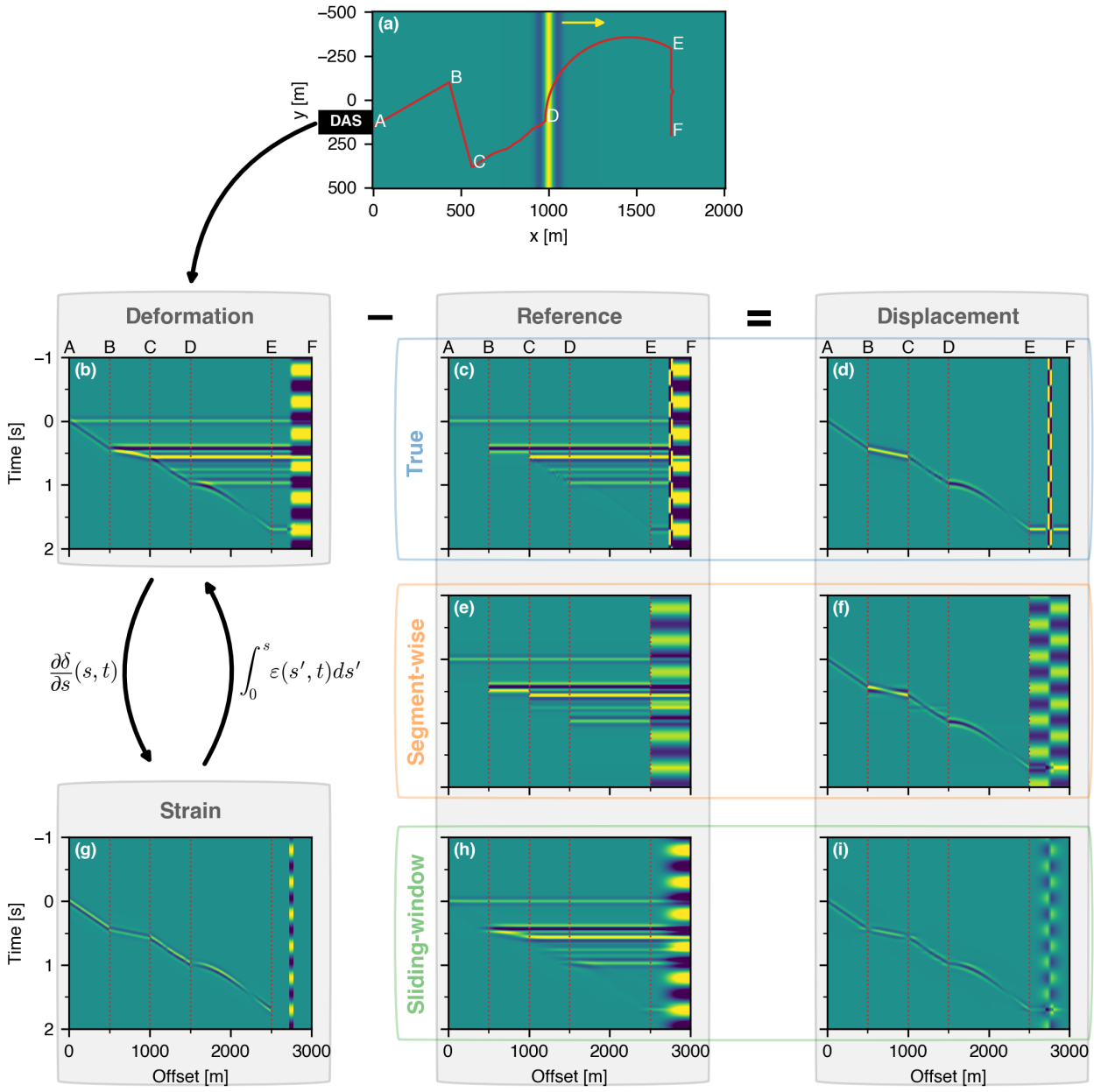

Figure S1. Same than Fig. 1 but for a plane S-wave. Similar results are observed meaning that the developed theory applies to both fundamental propagation modes in solids: longitudinal and shear waves.

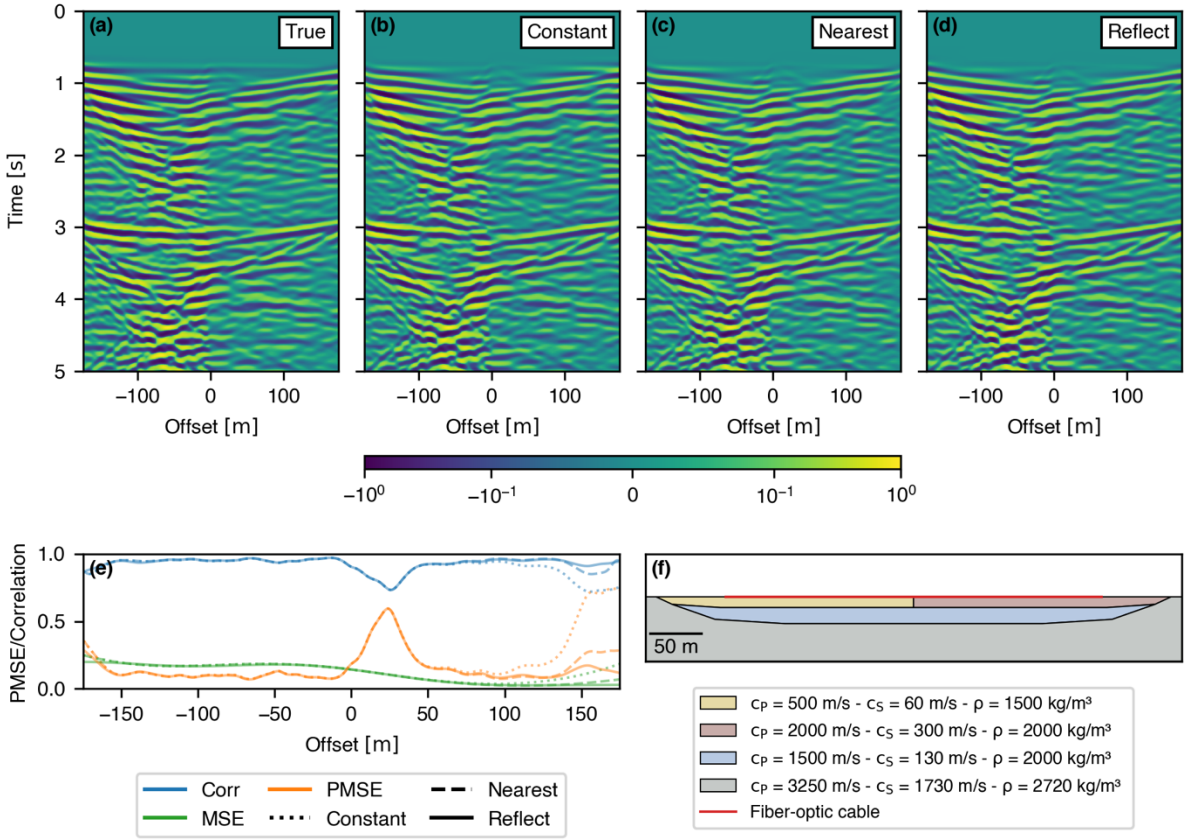

Figure S2. Effects of different padding modes used in the sliding-window scheme. The true velocity (a) is compared with recovered velocity using: (b) constant zero padding, (c) constant closest value padding, and, (d) reflection (or mirror) symmetric padding. Results are mostly identical except at the cable ends. (e) Error metrics for each padding mode. The reflect mode has overall better performances for this case.

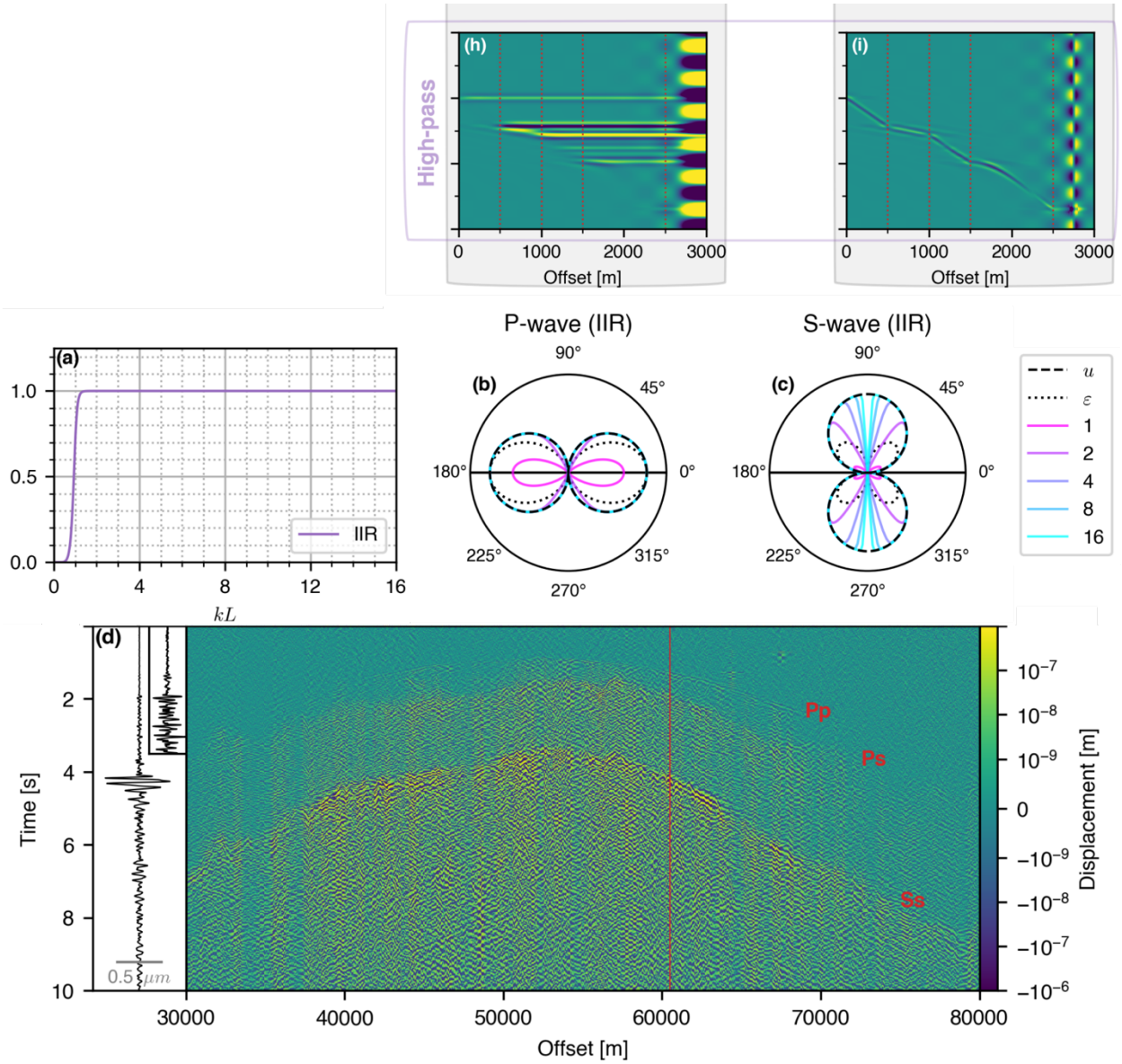

Figure S3. Infinite Impulse Response (IIR) method taken from (Yang et al., 2022) and applied to most figures of this study for comparison. A four-order high-pass Butterworth filter can be applied forward and backward along the spatial dimension (resulting in an eight-order filter) to perform an equivalent of the sliding-window-method with the same cut-off wavenumber. It works similarly in the sense that the filter is zero-phase and removes low wavenumber components, but some differences can be noted. (h & i) Same than Fig 1. In the illustrative simulation spatial leakage is easily observed and is due to the poor locality of the IIR method. (a) Same than Fig 3. The response of this method implies a steeper roll-off with lower sensitivity to low apparent wavenumbers compared to the sliding-window method with Hann taper. (b & c) This can also be observed on directivity patterns. (d) Same than Fig. 7. On real data the IIR method gives comparable results. It should be noted that IIR filters are less computationally intensive.

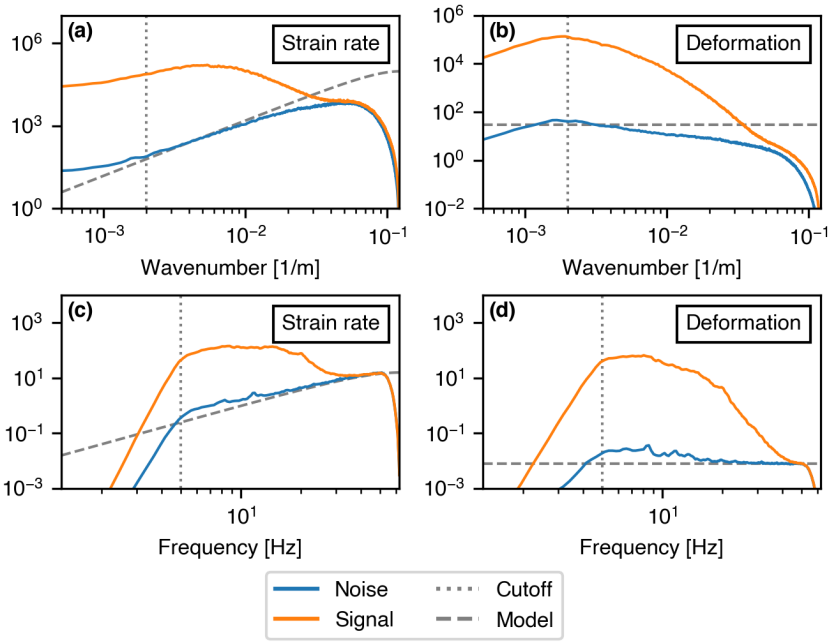

Figure S4. Noise levels of the OptoDAS interrogator. (a) Average raw strain rate levels in the wavenumber domain for 20 s time windows before (noise in blue) and during (signal in orange) the event presented in Fig 7. (b) Same but for the recovered displacement with a cut-off (vertical dotted grey line) wavelength of 500 m associated with the sliding 1 km Hann window used. (c) Raw strain rate levels but in the frequency domain with a clear cut-off frequency of 5 Hz implied by the filtered meant to remove the micro-seismic noise. (d) Same for the deformation-recovered displacement. The strain-rate noise level both increases with the wavenumber and the frequency but less than expected (grey dashed line). If noise was an additive white term in deformation and if strain-rate was computed by simple spatial and temporal differentiation we would expect linearly. It is probable that other derivation schemes are used, that the noise characteristic in deformation is not white and that more advances proprietary processing technics are used.